Complete Lyapunov Functions: Determination of the Chain-recurrent set using the Gradient*

Carlos Argáez[1 [0000−0002−0455−8015]], Peter Giesl[2 [0000−0003−1421−6980]] and Sigurdur Freyr Hafstein[1 [0000−0003−0073−2765]]

[1] Science Institute, University of Iceland, Dunhagi 5, 107 Reykjavík, Iceland
[2] University of Sussex, Falmer, BN1 9QH, United Kingdom
{carlos,shafstein}@hi.is, P.A.Giesl@sussex.ac.uk

Abstract. Complete Lyapunov functions (CLF) are scalar-valued functions, which are non-increasing along solutions of a given autonomous ordinary differential equation. They separate the phase-space into the chain-recurrent set, where the CLF is constant along solutions, and the set where the flow is gradient-like and the CLF is strictly decreases along solutions. Moreover, one can deduce the stability of connected components of the chain-recurrent set from the CLF.
While the existence of CLFs was shown about 50 years ago, in recent years algorithms to construct CLFs have been designed to determine the chain-recurrent set using the orbital derivative. These algorithms require iterative methods that constructed better and better approximations to a CLF, based on previous iterations. A drawback of these methods is the overestimation of the chain-recurrent set, which has been addressed by different methods.
In this paper, we construct a CLF using the previous method, but in contrast to previous work we will use the norm of the gradient of the computed CLF, rather than its orbital derivative, to determine the chain-recurrent set. We will show in this paper that this new approach determines the chain-recurrent set very well without the need of iterations or further methods to reduce the overestimation.

Keywords: Complete Lyapunov functions · chain-recurrent set · dynamical systems

1 Introduction

In this paper we study the dynamics of a general time-autonomous system of differential equations, given by (1),

$$\dot{\mathbf{x}} = \mathbf{f}(\mathbf{x}), \tag{1}$$

where $\mathbf{x} \in \mathbb{R}^n$ and $n \in \mathbb{N}$. We assume that $\mathbf{f} : \mathbb{R}^n \to \mathbb{R}^n$ is a continuously differentiable vector field and $\dot{\mathbf{x}}$ denotes the derivative with respect to time.

A solution $\mathbf{x}(t)$ to (1) with initial value ξ is a continuously differentiable function that satisfies the ODE (1) and such that $\mathbf{x}(0) = \xi$; if the solution is defined for all $t \in \mathbb{R}$, then this defines a dynamical system through $S_t\xi = \mathbf{x}(t)$.

* The first author in this paper is supported by the Icelandic Research Fund (Rannís), Iceland grant number 1163074-052, Complete Lyapunov functions: Efficient numerical computation.

Since analytical solutions to initial value problems are usually not obtainable, one could attempt to use numerical methods for a large collection of initial conditions for (1). This is computationally demanding, would only represent particular solutions, and might not reveal the general behaviour of the dynamical system over the whole phase space.

Special solutions of (1) are equilibria, i.e. points $\mathbf{x}_0$ with $\mathbf{f}(\mathbf{x}_0) = 0$, implying that the solution starting at the equilibrium will not change in time, but is a constant solution.

An equilibrium point is called stable if solutions starting at all adjacent points remain close for all future times. It is called attractive if all adjacent solutions will converge to it as time grows. That means that for an attractive equilibrium $\mathbf{x}_0$ one can find an open ball $B_\delta(\mathbf{x}_0)$ centered at $\mathbf{x}_0$ and with radius $\delta > 0$, such that $\|S_t\mathbf{x} - \mathbf{x}_0\| \to 0$ as $t \to \infty$ for all $\mathbf{x} \in B_\delta(\mathbf{x}_0)$. In this case, we can define the basin of attraction of $\mathbf{x}_0$ by $A(\mathbf{x}_0) = \{\mathbf{x} \in \mathbb{R}^n \mid S_t\mathbf{x} \to \mathbf{x}_0 \text{ as } t \to \infty\}$. The attractivity and stability are two different concepts and do not imply one another, however, when both occur, then we talk about an asymptotically stable equilibrium.

An asymptotically stable equilibrium is the simplest example of an attractor. An (local) attractor is a compact, invariant set, that attracts a neighborhood of itself. Further examples include asymptotically stable periodic orbits.

One method to analyse dynamical systems is to find the boundaries of the attractors' basins of attraction. A collection of methods exist to that aim. Among them, one can point out computing the invariant manifolds which form the boundaries of the attractors' basins of attraction [23]. Another well-known methodologies are set oriented methods [16] or the cell mapping approach [19]. All these methods require large computational effort.

An attractor and its basin of attraction can be characterised by a Lyapunov function, [24], originally introduced by Aleksandr Mikhailovich Lyapunov in 1893. A Lyapunov function is a scalar-valued function that attains its minimum on the attractor. Furthermore, its domain is the basin of attraction and it is strictly decreasing along all solutions apart from those on the attractor, where it is constant. An example for a Lyapunov function is the energy in a dissipative physical system. The advantage of the Lyapunov function is that it describes the behaviour of the system without computing its explicit solutions. However, this function is only defined in the basin of attraction of one attractor and describes this subset of the phase space.

Even if the attractor is an equilibrium, it is hard to obtain a Lyapunov function. If the system under analysis is linear, then it is possible to obtain a quadratic Lyapunov function relatively easily. However, if the system is not linear then, in general, one requires numerical algorithms to construct a Lyapunov function, see [18].

A *complete Lyapunov function* is an extension of the classical Lyapunov function for one attractor. It is defined on the whole state space and was introduced in [14, 15, 20, 21]. A complete Lyapunov function characterises the complete qualitative behaviour of the dynamical system on the whole phase space and not just in a neighbourhood of one particular attractor. Therefore, it allows to describe the different basins of attraction for all attractors of the dynamical system. Furthermore, it divides the state-space into two disjoint areas: The gradient-like flow, where the system's trajectories flow through, and

the chain-recurrent set, where infinitesimal perturbations can make the system recurrent. These two areas describe fundamentally different behaviours.

The regions in which the system is recurrent or almost recurrent, in the sense that ε-trajectories that are arbitrarily close to true system's solutions are recurrent, are usually referred to as the chain-recurrent set. This set can be shown to equal the intersection of all attractors and all corresponding repellers; for a precise definition see, e.g. [14].

The dynamics outside of the chain-recurrent set are similar to a gradient system, i.e. a system (1) where the right-hand side $\mathbf{f}(\mathbf{x})$ is given by the gradient $\nabla U(\mathbf{x})$ of a function $U : \mathbb{R}^n \to \mathbb{R}$. This set includes the transient behaviour of the system.

The authors have developed an algorithm to construct CLFs (for further reading, please refer to [2, 4–6, 3, 8, 10, 12, 11]). Thus, we are able to identify the chain-recurrent set and the gradient-like flow. The algorithm constructs a CLF by approximating solutions of a linear PDE, fixing values of the orbital derivative. It starts by fixing the values of the orbital derivative to -1, however, this problem does not have a solution on the chain-recurrent set, where the orbital derivative must be zero. Hence, we iteratively adjust the values of the orbital derivative, using the information of the previous iteration. The chain-recurrent set is then characterised as the set of points, where the orbital derivative of the approximating function is zero or close to zero.

The algorithm often overestimates the chain-recurrent set, i.e. the area where the approximating function has orbital derivative close to zero is larger than the actual chain-recurrent set. We have recently proposed a general algorithm to reduce the overestimation using geometric properties [7, 9].

In this paper, however, we use a new method to determine the chain-recurrent set, using the norm of the gradient of the computed CLF. It turns out that this gives a much more accurate indication of the chain-recurrent set without the need of further iterations or further algorithms to reduce the overestimation, and is thus preferable to the previous method. However, it requires a dense evaluation grid, where the norm of the gradient needs to be evaluated.

Let us give an idea of why the norm of the gradient is a good indicator of the chain-recurrent set. Consider the simple ODE $\dot{x} = -x$. In this example, the chain-recurrent set consists of the equilibrium at the origin, which is an attractor. When computing the solution to the PDE $V'(x) = -1$, where $V'(x) = \nabla V(x)\dot{f}(x)$ denotes the orbital derivative, we find the solution

$$V(x) = \begin{cases} \ln x + c_+ & \text{if } x > 0 \\ \ln|x| + c_- & \text{if } x < 0 \end{cases}$$

with arbitrary constants $c_+, c_- \in \mathbb{R}$; note that V is not defined at the equilibrium. Its gradient is given by

$$\|\nabla V(x)\| = \frac{1}{|x|} \quad \text{if} \quad x \neq 0.$$

The mesh-free collocation method, which we use to approximate V, however, produces a smooth function $v(x)$, which fulfills the PDE in all given collocation points (which cannot includes the equilibrium) and minimises the norm in a certain Hilbert space. Moreover, if the fill distance of the collocation points converges to 0, i.e. they become denser and denser, then v converges to V, and the same holds for its gradient. This

means that $\|\nabla v(x)\|$ becomes very large for x is close to 0. However, since v is a smooth function and $\nabla v(x) \approx \frac{-1}{-x} = \frac{1}{x}$ changes sign at $x = 0$, we expect that $\|\nabla v(0)\| = 0$. Hence, the chain-recurrent set is characterised by the points x fulfilling the condition $\|\nabla v(x)\| \approx 0$, while close to it we have $\|\nabla v(x)\| \gg 1$. Note that the same behaviour occurs for a repeller; consider e.g. the system $\dot{x} = x$. The argument fails, however, for a non-hyperbolic equilibrium.

Let us give an overview of the contents of the paper: Section 2 contains a description of the construction of the Complete Lyapunov function and the computation of its gradient, as well as a description and pseudo-code on how the implementation is done. In Section we apply the method to several examples and compare our results to the previous method. In Section we discuss the results and give our conclusions.

2 Construction of Complete Lyapunov functions

2.1 Mesh-free collocation

Mesh-free collocation, in particular using Radial Basis Functions (RBFs), is a powerful method to solve (generalised) interpolation problems, e.g. linear PDEs [26, 13]. In particular, they can be used to construct CLFs when posed as a generalized interpolation problem.

RBFs are real-valued functions whose evaluation depends only on the norm of a point in $\mathbb{R}^n$. Common examples of RBFs are Gaussians and multiquadrics. In this paper, we use Wendland functions as RBF, which are compactly supported and positive definite functions [25]. They have the advantage of being expressed as algebraic polynomials on their compact support. Further, the corresponding Reproducing Kernel Hilbert Space H is norm-equivalent to a Sobolev space.

2.2 Wendland functions

The general form of a Wendland function [25] is $\psi(\mathbf{x}) := \psi_{l,k}(c\|\mathbf{x}\|)$, where $c > 0$ determines the size of the compact support and $k \in \mathbb{N}$ is a smoothness parameter. For our application the parameter l is fixed as $l = \lfloor \frac{n}{2} \rfloor + k + 1$. The Reproducing Kernel Hilbert Space corresponding to $\psi_{l,k}$ contains the same functions as the Sobolev space $W_2^{k+(n+1)/2}(\mathbb{R}^n)$ and the spaces are norm equivalent.

The functions $\psi_{l,k}$ are defined by the recursion: For $l \in \mathbb{N}$ and $k \in \mathbb{N}_0$, we define

$$\begin{aligned} \psi_{l,0}(r) &= (1-r)_+^l, \\ \psi_{l,k+1}(r) &= \textstyle\int_r^1 t\psi_{l,k}(t)\mathrm{d}t \end{aligned} \tag{2}$$

for $r \in \mathbb{R}_0^+$, where $x_+ = x$ for $x \geq 0$ and $x_+ = 0$ for $x < 0$. Note that $x_+^l := (x_+)^l$.

2.3 Collocation points

To construct a CLF for system (1), we use mesh-free collocation with RBFs. The method finds the norm-minimal function in the Reproducing Kernel Hilbert space, that

satisfies the PDE $V'(\mathbf{x}) = -1$ at all collocation points $\mathbf{x}$; this is a special type of a generalised interpolation problem. It turns out that the solution is a linear combination of the Riesz-representatives, which can easily be calculated in a Reproducing Kernel Hilbert space. The coefficients of the linear combination are determined by solving a system of linear equations, given by the so-called collocation matrix.

As collocation points, we use a subset, $X = \{\mathbf{x}_1, \ldots, \mathbf{x}_N\} \subset \mathbb{R}^n$, of a hexagonal grid with fineness-parameter $\alpha_{\text{Hexa-basis}} \in \mathbb{R}^+$ constructed according to the equation:

$$\begin{aligned} &\{\alpha_{\text{Hexa-basis}} \textstyle\sum_{k=1}^{n} i_k \omega_k : i_k \in \mathbb{Z}\}, \\ &\omega_k = \textstyle\sum_{j=1}^{k-1} \varepsilon_j \mathbf{e}_j + (k+1)\varepsilon_k \mathbf{e}_k \\ &\text{and } \varepsilon_k = \sqrt{\frac{1}{2k(k+1)}}. \end{aligned} \tag{3}$$

Here $\mathbf{e}_j$ is the usual jth unit vector. These basis vectors are shown in red colour in Figure 1 in $\mathbb{R}^2$, while the canonical vectors are shown in black. The hexagonal grid has

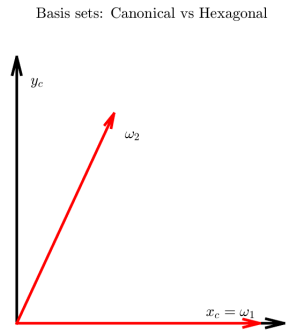

Fig. 1. Black: Canonical basis. Red: Hexagonal basis set. Image taken from [7].

been shown to minimize the condition numbers of the collocation matrices for a fixed fill distance, i.e. a measure of the density of the collocation grid [22]. The collocation points must not include any equilibrium, i.e. any point $\mathbf{x}$ with $\mathbf{f}(\mathbf{x}) = \mathbf{0}$. In fact, including an equilibrium in the set of collocation points X renders the collocation matrix singular.

Practically, we compute the solution v of the generalised interpolation problem $V'(\mathbf{x}) = -1$ by solving a system of N linear equations, where N is the number of collocation points.

$$\begin{aligned} v(\mathbf{x}) &= \textstyle\sum_{k=1}^{N} \beta_k \langle \mathbf{x}_k - \mathbf{x}, \mathbf{f}(\mathbf{x}_k)\rangle \psi_1(\|\mathbf{x} - \mathbf{x}_k\|), \\ v'(\mathbf{x}) &= \textstyle\sum_{k=1}^{N} \beta_k \Big[-\psi_1(\|\mathbf{x} - \mathbf{x}_k\|)\langle \mathbf{f}(\mathbf{x}), \mathbf{f}(\mathbf{x}_k)\rangle \\ &\qquad + \psi_2(\|\mathbf{x} - \mathbf{x}_k\|)\langle \mathbf{x} - \mathbf{x}_k, \mathbf{f}(\mathbf{x})\rangle \\ &\qquad \cdot \langle \mathbf{x}_k - \mathbf{x}, \mathbf{f}(\mathbf{x}_k)\rangle \Big], \end{aligned} \tag{4}$$

where ψ_1, ψ_2 are given by $\psi_j(r) = \frac{1}{r}\frac{d\psi_{j-1}(r)}{dr}$ for $r > 0$ and $j = 1,2$ and $\psi_0(r) = \psi_{l,k}$ is a Wendland function. Moreover, $\langle\cdot,\cdot\rangle$ denotes the standard scalar product and $\|\cdot\|$ the Euclidean norm in $\mathbb{R}^n$, $\beta \in \mathbb{R}^N$ is the solution to $A\beta = \mathbf{r}$, $r_k = r(\mathbf{x}_k)$ and A is the $N \times N$ matrix with entries

$$\begin{aligned} a_{ij} = \psi_2(\|\mathbf{x}_i - \mathbf{x}_j\|)\langle \mathbf{x}_i - \mathbf{x}_j, \mathbf{f}(\mathbf{x}_i)\rangle\langle \mathbf{x}_j - \mathbf{x}_i, \mathbf{f}(\mathbf{x}_j)\rangle \\ -\psi_1(\|\mathbf{x}_i - \mathbf{x}_j\|)\langle \mathbf{f}(\mathbf{x}_i), \mathbf{f}(\mathbf{x}_j)\rangle \end{aligned} \tag{5}$$

for $i \neq j$ and

$$a_{ii} = -\psi_1(0)\|\mathbf{f}(\mathbf{x}_i)\|^2.$$

More detailed explanations on this construction are given in [17, Chapter 3]. If no collocation point $\mathbf{x}_j$ is an equilibrium for the system, i.e. $\mathbf{f}(\mathbf{x}_j) \neq \mathbf{0}$ for all j, then the matrix A is positive definite and the system of equations $A\beta = \mathbf{r}$ has a unique solution.

The last assertion will hold true independently of whether the underlying discretized PDE has a solution or not, while error estimates are obviously only available if the PDE has a solution.

As it can be seen in equations (4), we use two set of points: $\mathbf{x}_j$ that represent the collocation points and $\mathbf{x}$ that represent the evaluation points. If we evaluate the approximation v at a collocation point $\mathbf{x}_j$ we have $v'(\mathbf{x}_j) = -1$ by construction. If the PDE has a solution, then error estimates ensure that $V'(\mathbf{x})$ and $v'(\mathbf{x})$ are close if the collocation points are sufficiently dense. However, as the PDE has no solution at points of the chain-recurrent set, these error estimates are not applicable. In previous work the values of $v'(\mathbf{x})$ were used for subsequent iterations of the method and thus each evaluation point was associated with an appropriate collocation point [2, 4, 8, 5]. In particular, the first approximation v to a CLF is given by a function which satisfies the PDE $v'(\mathbf{x}) = -1$ at all collocation points and is norm minimal in the corresponding Reproducing Kernel Hilbert space H. In later iterations we solve $v'(\mathbf{x}) = r_j$ for different $r_j \leq 0$, determined by previous approximations.

However, in this paper we do not need to reiterate on previous approximations. It will be shown that to have a good approximation to the chain-recurrent set, it is sufficient to find the function that satisfies the PDE $v'(\mathbf{x}) = -1$ at all collocation points. In this paper, we use a dense Cartesian evaluation grid, namely a finite subset of $h\mathbb{Z}^n$ with small $h > 0$. The cardinality of the evaluation grid is denoted by Ξ.

As introduced and explained in [4] it is advantageous to use an "almost" normalized approach, i.e., replace the original dynamical system (1) by

$$\dot{\mathbf{x}} = \hat{\mathbf{f}}(\mathbf{x}), \quad \text{where} \quad \hat{\mathbf{f}}(\mathbf{x}) = \frac{\mathbf{f}(\mathbf{x})}{\sqrt{\delta^2 + \|\mathbf{f}(\mathbf{x})\|^2}} \tag{6}$$

with a small parameter $\delta > 0$. This new system has the same trajectories as the original one, but the speed with which trajectories are passed through is more uniform, i.e. $\|\hat{\mathbf{f}}(\mathbf{x})\| \approx 1$ if $\mathbf{x}$ is not an equilibrium. This normalization already reduces significantly the overestimation of the chain-recurrent set.

2.4 Gradient of v

The gradient of a function $v(x_1, \ldots, x_n)$, is the vector field defined as

$$\nabla v(x_1,\ldots,x_n) = \left(\frac{\partial \mathbf{v}}{\partial x_1}(x_1,\ldots,x_n),\ldots,\frac{\partial \mathbf{v}}{\partial x_n}(x_1,\ldots,x_n) \right).$$

As explained in the introduction, in this paper we will use the criterion $\nabla \mathbf{v}(x_1,\ldots,x_n) \approx 0$ to determine the points in the chain-recurrent set. In practice, we will choose a small parameter γ_2 and determine the points $\mathbf{x} = (x_1,\ldots,x_n)$ with $\|\nabla v(\mathbf{x})\| \leq \gamma_2$.

Therefore, we calculate the first derivative of the function v, see (4), as:

$$\begin{aligned}\frac{\partial v}{\partial x_i}(\mathbf{x}) &= \sum_{k=1}^{N} \beta_k \frac{\partial}{\partial x_i}((\mathbf{x}_k-\mathbf{x})^T \mathbf{f}(\mathbf{x}_k)\psi_1(\|\mathbf{x}-\mathbf{x}_k\|)) \\ &= \sum_{k=1}^{N} \beta_k \left[-f_i(\mathbf{x}_k)\psi_1(\|\mathbf{x}-\mathbf{x}_k\|) + (\mathbf{x}-\mathbf{x}_k)_i(\mathbf{x}_k-\mathbf{x})^T \mathbf{f}(\mathbf{x}_k)\psi_2(\|\mathbf{x}-\mathbf{x}_k\|)\right]\end{aligned}$$

Code In this section, we explain the algorithm used to compute the gradient. Our code is a continuation of the published, free-distributed code, LyapXool [11].

```
for j=1:Ξ
  for k=1:N
     for i=1:n
          ∇v(j,i)+ = β(k) * (−f̂_i(x_k) * ψ1(‖y_j − x_k‖)
                                  +(y_j − x_k)_i * (x_k − y_j)^T f̂(x_k) * ψ2(‖y_j − x_k‖)
     end
  end
end
```

Here $\nabla v(j,i)$ is the ith component of the gradient of v at the evaluation point $\mathbf{y}_j$ and we use the collocation points $\mathbf{x}_k$, $k = 1,2,\ldots,N$. As it can be seen, the computation of the gradient vector is a factor n more workload than just computing the CLF and its orbital derivative, which previously was analysed in [8].

3 Results

We approximate the solution of $V'(\mathbf{x}) = -1$ by v, using the collocation points X. Previously, when we analysed the orbital derivative, we defined a tolerance parameter $-1 < \gamma_1 \leq 0$, and marked a collocation point $\mathbf{x}_j$ to be poorly approximated, i.e., an element of our approximation of the chain-recurrent set ($\mathbf{x}_j \in X^0$), if there is at least one point $\mathbf{x}$ associated to the point $\mathbf{x}_j$, i.e. near to $\mathbf{x}_j$, such that $v(\mathbf{x}) > \gamma$. The well approximated points, i.e., for which the condition $v'(\mathbf{x}) < \gamma$ holds for all $\mathbf{x}$ near $\mathbf{x}_j$ belong to our approximation of the area of the gradient-like flow ($\mathbf{x} \in X^-$).

Now we look for points in the evaluation grid such that $\|\nabla v(\mathbf{x})\| \approx 0$, so we define $0 < \gamma_2$ and a collocation point $\mathbf{x}_j$ such that $\|\nabla v(\mathbf{x})\| \leq \gamma$ for some evaluation point $\mathbf{x}$ associated to $\mathbf{x}_j$ is considered to belong to X^0. In the following, we compare the results of our new method with those of the previous one for several examples.

3.1 Two orbits

Consider the system (1) with

$$\mathbf{f}(x,y) = \begin{pmatrix} -x(x^2+y^2-1/4)(x^2+y^2-1)-y \\ -y(x^2+y^2-1/4)(x^2+y^2-1)+x \end{pmatrix}. \tag{7}$$

This system has an asymptotically stable equilibrium at the origin and two periodic circular orbits: an asymptotically stable periodic orbit at $\Omega_1 = \{(x,y) \in \mathbb{R}^2 \mid x^2+y^2 = 1\}$ and a repelling periodic orbit at $\Omega_2 = \{(x,y) \in \mathbb{R}^2 \mid x^2+y^2 = 1/4\}$.

To compute the CLF we used the Wendland function $\psi_{4,2}$. The collocation points were set in a region $[-1.5,1.5] \times [-1.5,1.5] \subset \mathbb{R}^2$ and we used a hexagonal grid (3) with $\alpha_{Hexa-basis} = 0.0131$. We computed this example with the almost-normalized method $\dot{\mathbf{x}} = \hat{\mathbf{f}}(\mathbf{x})$ with $\delta^2 = 10^{-8}$. Figure 2 shows the function v, displaying a maximum at the repelling periodic orbit and minima at the attractive periodic orbit as well as the asymptotically stable equilibrium at the origin. Figure 3 shows the orbital derivative v', which is -1 by construction apart from the points in the chain-recurrent set.

Using the previous method, namely the orbital derivative, the chain-recurrent set is obtained by choosing the points satisfying $v'(\mathbf{x}) \geq \gamma_1$ with the critical parameter $\gamma_1 = -0.25$, see Figure 4 where the failing points of the evaluation grid are plotted.

Using our new method, we determine the chain-recurrent set as points satisfying $\|\nabla v(\mathbf{x})\| \leq \gamma_2$ with $\gamma_2 = 0.9$. Figures 5 and 6 display the norm of the gradient and Figure 7 shows the points satisfying $\|\nabla v(\mathbf{x})\| \leq \gamma_2$ with $\gamma_2 = 0.9$. The evaluation grid was computed with the Cartesian grid with a distance parameter $h = 0.0007$. For this example, $N = 60,456$ and $\Xi = 18,369,796$.

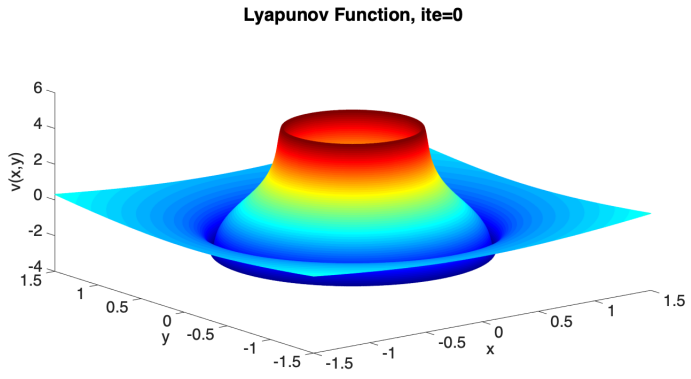

Fig. 2. Complete Lyapunov function for system (7). It clearly shows two orbits and one attractor at the origin.

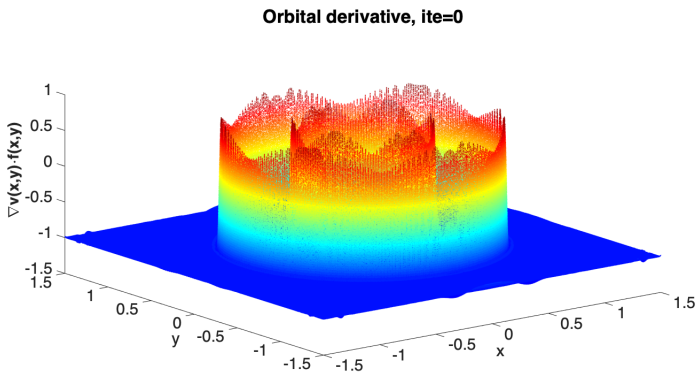

Fig. 3. Orbital derivative for system (7). As it is seen, all points in the gradient-like flow satisfy the condition -1.

The CLF, Figure 2, approximated by our method for system (4) shows a system whose behaviour has two circular period orbits with $r_1 = 1/2$ and $r_2 = 1$. Furthermore, the presence of an attractor at the origin is clear. Figure 3 shows that the condition -1 is satisfied for all points in the gradient-like flow while the values of the orbital derivative over the chain-recurrent set are clearly different. Points with an orbital derivative larger than $\gamma = -0.25$ give us our first approximation to the chain-recurrent set, Figure 4. All components of the chain-recurrent set, the equilibrium and the two periodic orbit, are present, but the periodic orbits are over-estimated. That overestimation was reduced using geometrical properties in [7].

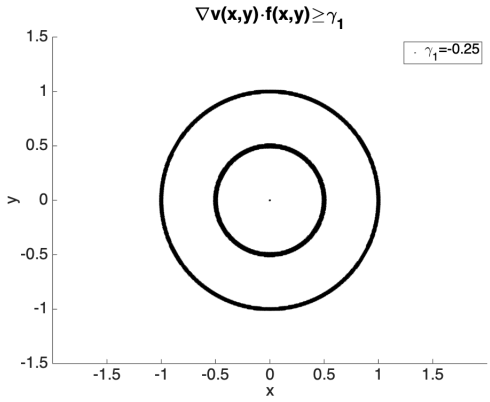

Fig. 4. Chain-recurrent set for system (7) constructed by filtering the orbital derivative. Two orbits are seen at $r = 1$ and $r = 1/2$. The attractive origin is also found. The critical value to filter the orbital derivative was $\gamma_1 = -0.25$.

Let us now discuss the norm of the gradient of the CLF, see Figure 5. As discussed in the introduction, the norm is very large close to the chain-recurrent set, and close to 0 directly on the chain-recurrent set, cf. Figure 6

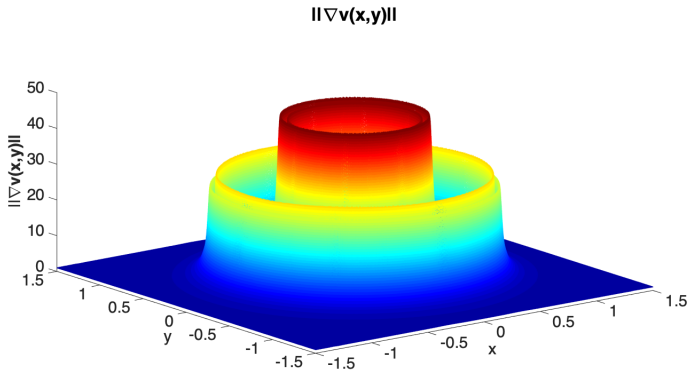

Fig. 5. Norm of the gradient of v for system (7).

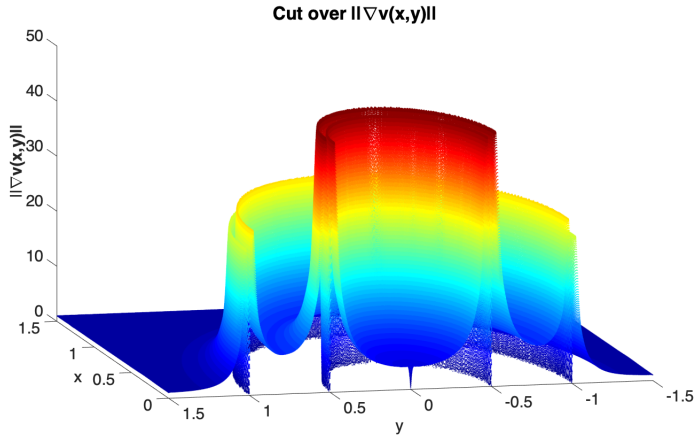

Fig. 6. Norm of $\|\nabla v\|$ for system (7). As it can be see, the figure has been cut to show the behaviour close the chain-recurrent set.

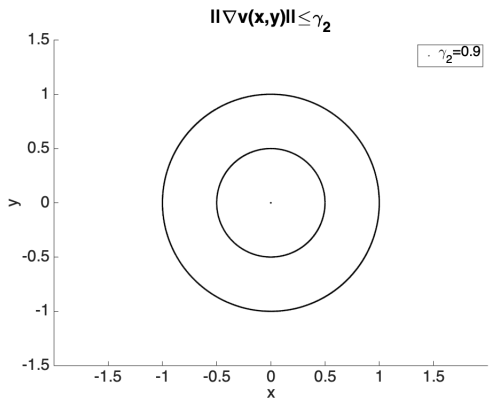

Fig. 7. Chain-recurrent set for system (7) constructed by filtering the norm of the gradient of the Lyapunov Function. Two orbits are seen at $r = 1$ and $r = 1/2$. The attractive origin is also found. The critical value to filter the orbital derivative was $\gamma_2 = 0.9$.

Figure 7 shows the points with norm $\|\nabla v(\mathbf{x})\| \leq \gamma_2$ and displays precisely the same two orbits and the critical point. In this case, however, the norm of the gradient vector of v was used instead of the orbital derivative. Compared to the previous method, see Figure 4, the new method shows the chain-recurrent set much sharper and with hardly any overestimation. A direct comparison between the two sets is shown in Figure 8.

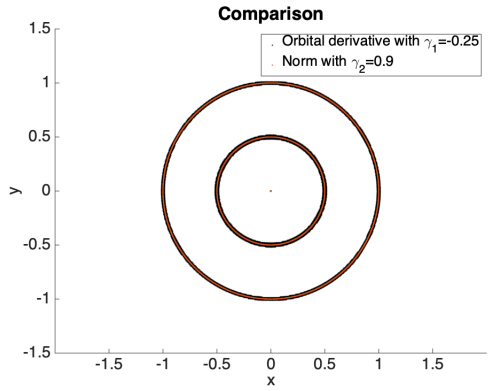

Fig. 8. Chain-recurrent set for system (7). Black: using the orbital derivative (previous method). Red: using the gradient of the complete Lyapunov function (new method).

Figure 8 reveals how much the old method overestimates the chain-recurrent set in comparison to the new method.

3.2 Van der Pol oscillator

The Van der Pol oscillator is a classical example in dynamical systems. It is represented by equation (8).

$$\begin{pmatrix} \dot{x} \\ \dot{y} \end{pmatrix} = \mathbf{f}(x,y) = \begin{pmatrix} y \\ (1-x^2)y - x \end{pmatrix}. \tag{8}$$

For computing the CLF associated to system (8), we set $\alpha_{\text{Hexa-basis}} = 0.027$ over the area defined by $[-3,3]^2 \subset \mathbb{R}^2$. As before we use the almost normalized method with $\delta^2 = 10^{-8}$. The Wendland function used is $\psi_{4,2}$ and we have used the critical values $\gamma_1 = -0.25$ for the orbital derivative and $\gamma_2 = 0.9$ for the norm of the gradient. The evaluation grid was computed with the Cartesian grid with a distance parameter $h = 0.0015$. For this example, $N = 61,446$ and $\Xi = 16,008,001$.

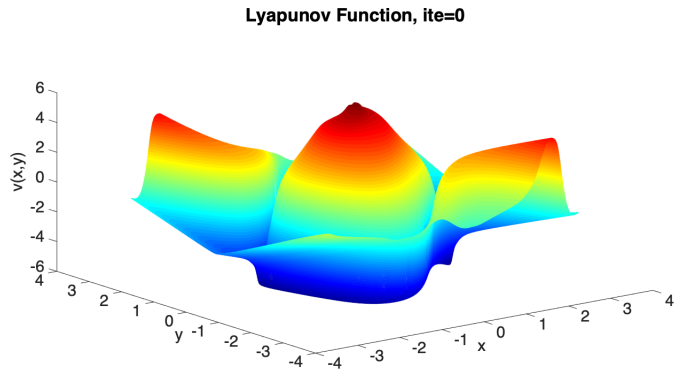

Fig. 9. Complete Lyapunov function for system (8). The repeller at the origin and the attractive periodic orbit are clearly seen.

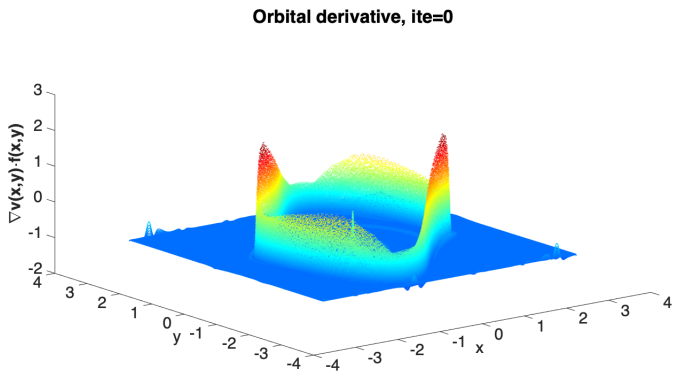

Fig. 10. Orbital derivative for system (8).

Figures 9 and 10 show the computed CLF and its orbital derivative associated to the system (8). Again, we can see that the behaviour of this system is represented clearly by the CLF – it has a minimum at the periodic orbit and a maximum at the unstable equilibrium at the origin. As well, the orbital derivative is -1 at all point in the gradient-like flow, while being larger on the chain-recurrent set.

The chain-recurrent set obtained by plotting the points where the orbital derivative satisfies $v'(\mathbf{x}) \geq \gamma_1$ is shown in Figure 11.Again the periodic orbit for this system is clearly overestimated.

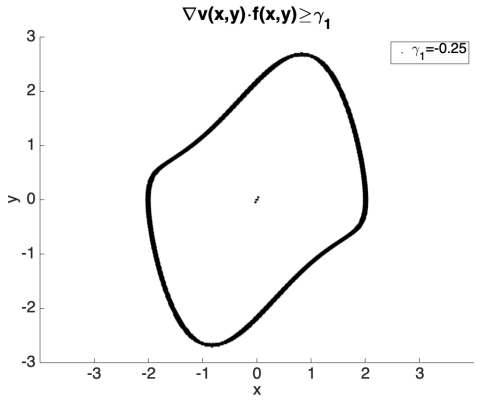

Fig. 11. Chain-recurrent set for system (8) obtained by the orbital derivative.

Figure 12 displays the norm of the gradient of the CLF. Near the periodic orbit the norm is again very large, while it is close to zero on the periodic orbit. The chain-recurrent set obtained by plotting the points with $\|\nabla v(\mathbf{x})\| \leq \gamma_2$ is shown in Figure 13.

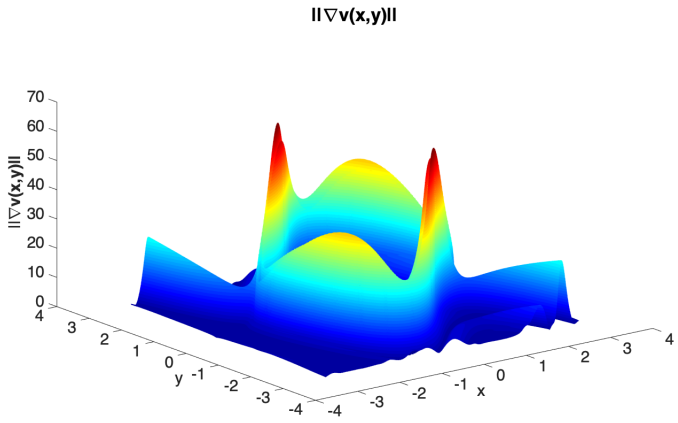

Fig. 12. Norm of the gradient of v for system (8).

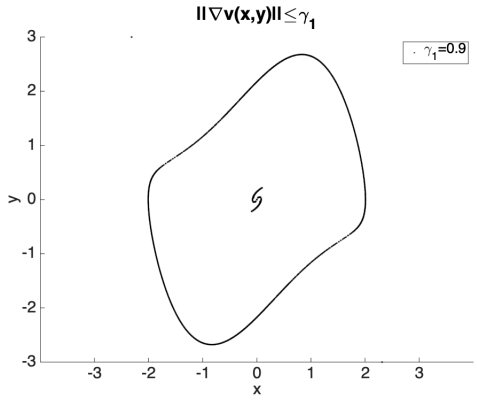

Fig. 13. Chain-recurrent set for system (8) obtained by the norm of the gradient.

As is clearly seen in Figure 13, the chain-recurrent set obtained with the norm of the gradient of v is sharper around the periodic orbit; it is not fully closed, but the shape is clearly visible. However, there is overestimation around the equilibrium, which will be addressed in Section 4.

3.3 Homoclinic orbit

In dynamical systems, a homoclinic orbit is a trajectory which connects an equilibrium to itself. In this paper, we consider the following system with a homoclinic orbit,

$$\begin{pmatrix}\dot{x}\\ \dot{y}\end{pmatrix} = \mathbf{f}(x,y) = \begin{pmatrix}x(1-x^2-y^2)-y((x-1)^2+(x^2+y^2-1)^2)\\ y(1-x^2-y^2)+x((x-1)^2+(x^2+y^2-1)^2)\end{pmatrix}. \tag{9}$$

For this system, the origin is an unstable focus. The system has an asymptotically stable homoclinic orbit at a circle centred at the origin and with radius 1, connecting the equilibrium $(1,0)$ with itself. We used the Wendland function $\psi_{4,2}$ for our computations.

The collocation points were set in a region $[-1.5,1.5]\times[-1.5,1.5]\subset\mathbb{R}^2$ and we used a hexagonal grid (3) with $\alpha_{\mathrm{H}exa-basis} = 0.0131$. We computed this example with the almost-normalized method $\dot{\mathbf{x}} = \hat{\mathbf{f}}(\mathbf{x})$ with $\delta^2 = 10^{-8}$. We used the following critical values: $\gamma_1 = -0.25$ for the orbital derivative and $\gamma_2 = 0.9$ for the norm of the gradient. The evaluation grid was computed with the Cartesian grid with a distance parameter $h = 0.0007$. For this example, $N = 60,456$ and $\Xi = 18,369,796$.

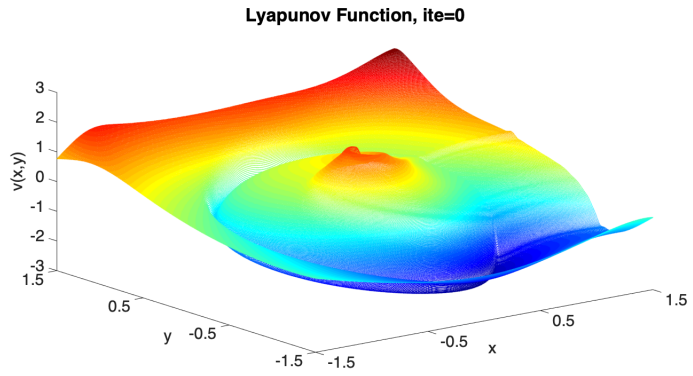

Fig. 14. Complete Lyapunov function for system (9).

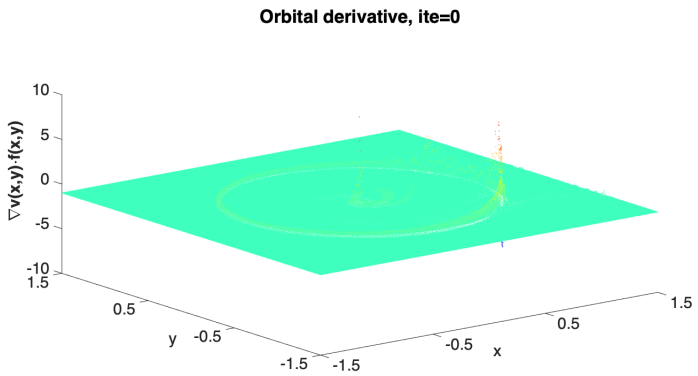

Fig. 15. Orbital derivative of the complete Lyapunov function for system (9). It clearly shows how the approximation to -1 succeeds over the gradient-like flow while it fails over the chain-recurrent set.

Figures 14 and 15 show a CLF and its orbital derivative associated to system (9). Again, the system's behaviour is represented clearly by the CLF. The function satisfies the condition $v'(\mathbf{x}) \approx -1$ at all point in the gradient-like flow, while this fails over the chain-recurrent set.

The chain-recurrent set obtained by the orbital derivative is shown in Figure 16 for failing points of the evaluation grid.

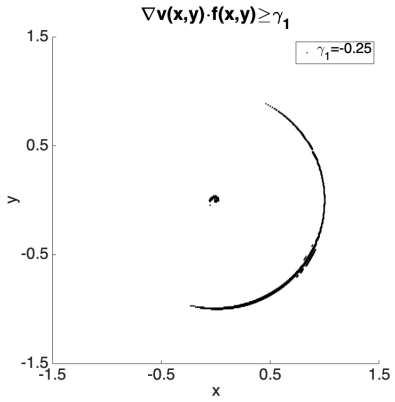

Fig. 16. Chain-recurrent set for system (9) obtained by the orbital derivative.

Unlike the previous examples, this system is rather complicated. Plotting the points with orbital derivative $v'(\mathbf{x}) \leq \gamma_1 = -0.25$ does not sufficiently classify the orbit; some parts are overestimated and some are missing. Using a γ_1 closer to -1, as done in [2, 4,

5, 8], helps to fully determine the homoclinic orbit. However, that will also bring more overestimation.

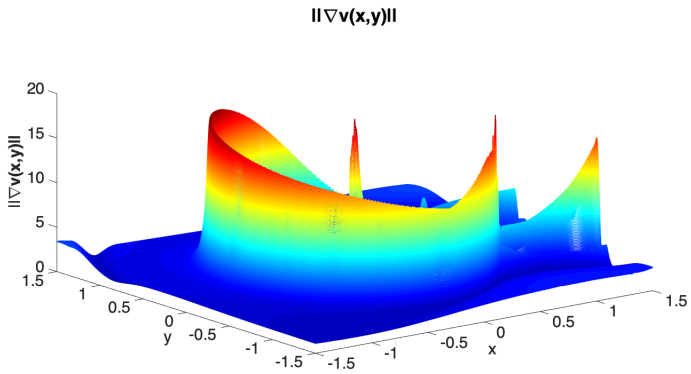

Fig. 17. Norm of the gradient of v for system (9).

Figure 17 displays norm of the gradient of the CLF, while Figure 18 shows the chain-recurrent set obtained through the gradient of the CLF.

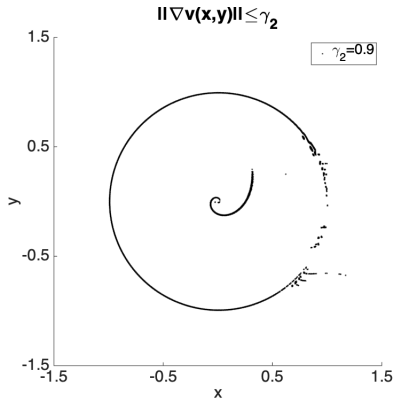

Fig. 18. Chain-recurrent set for system (9) obtained by the gradient.

As for the system (8), this orbit is not closed either. However, it is sufficiently well-defined. The overestimation is minor on the orbit and even if it is considerable around the equilibrium, that is not an issue as discussed in Section 4.

4 Discussion

The new method, using the norm of the gradient to classify the chain-recurrent set, gives sharper image of the chain-recurrent set, i.e. it has less overestimation. Further, it misses less parts of it. These results have been obtained without iterations. The determination of equilibria and higher-dimensional sets in the chain-recurrent set requires two different critical values; this was observed for the previous method in [12], where we have discussed the problem of finding appropriate critical values for the chain-recurrent set when using the orbital derivative. As is explained in [12], we should consider two different critical values, one for orbits and another for equilibrium points. Indeed, for a system (1) the equilibrium points can be computed by solving $\mathbf{f}(\mathbf{x}) = 0$, often analytically. For these reasons, in this paper we have focused on classifying the orbits.

The new method requires higher computational effort when compared to one iteration of the previous one: first, we require a dense evaluating – this is related to the fact that the norm of the gradient is only close to zero on a very small set. Indeed, the norm of the gradient becomes large close to the area where it is small! However, this also delivers a sharp resolution of the chain-recurrent set. In future work we intend to first use a course evaluation grid and then refine it locally in areas of interest. Second, the computation of the gradient, as explained in Section 2.4, is computationally more costly by factor n.

5 Conclusions

We have introduced a new method to determine the chain-recurrent set of dynamical systems using approximations to complete Lyapunov functions. While previous methods determined the chain-recurrent set by finding points where the orbital derivative of the complete Lyapunov functions is close to zero, i.e. $v'(\mathbf{x}) \approx 0$, the new method uses the norm of its gradient and determines points where $\|\nabla v(\mathbf{x})\| \approx 0$. The new method is able to determine the chain-recurrent set better, both by detecting all areas and by reducing its overestimation. The method will be extended in the future in order to automatically determine stable and unstable components of the chain-recurrent set, as well as stable and unstable directions by determining minima and maxima of the function v.

References

1. Anderson, J. and Papachristodoulou, A. (2015). Advances in computational Lyapunov analysis using sum-of-squares programming. *Discrete Contin. Dyn. Syst. Ser. B*, 20(8):2361–2381.
2. Argáez, C., Giesl, P., and Hafstein, S. (2017a). Analysing dynamical systems towards computing complete Lyapunov functions. *Proceedings of the 7th International Conference on Simulation and Modeling Methodologies, Technologies and Applications*. SIMULTECH 2017, Madrid, Spain.
3. C. Argáez, P. Giesl, and S. Hafstein, (2018a) *Computation of complete Lyapunov functions for three-dimensional systems. In: Proceedings of the 57rd IEEE Conference on Decision and Control (CDC)*, Miami Beach, FL, USA, 2018, pp. 4059-4064

4. Argáez, C., Giesl, P., and Hafstein, S. (2018b). Computational approach for complete Lyapunov functions. *In Dynamical Systems in Theoretical Perspective, Springer Proceedings in Mathematics and Statistics 248*, Springer 2018. pp. 1-11.
5. Argáez, C., Giesl, P. and Hafstein, S. (2018c) Iterative Construction of Complete Lyapunov Functions. DOI: 10.5220/0006835402110222 *In Proceedings of 8th International Conference on Simulation and Modeling Methodologies, Technologies and Applications (SIMULTECH 2018)*, pages 211-222 ISBN: 978-989-758-323-0
6. Argáez, C., Giesl, P. and Hafstein, S. (2018d) Construction of a Complete Lyapunov Function using Quadratic Programming. *In Proceedings of the 15th International Conference on Informatics in Control, Automation and Robotics (ICINCO)*, Porto, Portugal, 2018, pp. 560-568.
7. Argáez, C., Giesl, P. and Hafstein, S. (2019a) Middle Point Reduction of the Chain-recurrent Set. *In: Proceedings of the 9th International Conference on Simulation and Modeling Methodologies, Technologies and Applications (SIMULTECH)*, Prague, Czech Republic, 2019, pp. 141-152.
8. Argáez, C., Giesl, P. and Hafstein, S. (2019b) Complete Lyapunov Functions: Computation and Applications. *In: Simulation and Modeling Methodologies, Technologies and Applications Series: Advances in Intelligent Systems and Computing 873*, Springer 2019. pp. 200-221.
9. Argáez, C., Giesl, P. and Hafstein, S. (2019c) Clustering Algorithm for Generalized Recurrences using Complete Lyapunov Functions. *In: Proceedings of the 16th International Conference on Informatics in Control, Automation and Robotics (ICINCO)*, Prague, Czech Republic, 2019, pp. 138-146.
10. Argáez, C., Giesl, P. and Hafstein, S. (2019d) Improved estimation of the chain-recurrent set. *In: Proceedings of the 18th European Control Conference (ECC)*, Napoli, Italy, 2019, pp. 1622-1627.
11. Argáez, C., Berthet, J.-C., Björnsson, H., Giesl, P. and Hafstein, S. (2019e) LyapXool - a program to compute complete Lyapunov functions *SoftwareX*,ISSN: 2352-7110, Vol: 10, Page: 100325
12. Argáez, C., Giesl, P. and Hafstein, S. (2019f) Critical tolerance evolution: Classification of the chain-recurrent set In DSTA 2019, (To be published)
13. Buhmann, M. (2003). Radial basis functions: theory and implementations. Cambridge University Press, Cambridge.
14. Conley, C. (1978a). *Isolated Invariant Sets and the Morse Index*. CBMS Regional Conference Series no. 38. American Mathematical Society.
15. Conley, C. (1988). The gradient structure of a flow I. *Ergodic Theory Dynam. Systems*, 8:11–26.
16. Dellnitz, M. and Junge, O. (2002). Set oriented numerical methods for dynamical systems. In *Handbook of dynamical systems, Vol. 2*, pages 221–264. North-Holland, Amsterdam.
17. Giesl, P. (2007). *Construction of Global Lyapunov Functions Using Radial Basis Functions*. Lecture Notes in Math. 1904, Springer.
18. Giesl, P. and Hafstein, S. (2015). Review on computational methods for Lyapunov functions. *Discrete Contin. Dyn. Syst. Ser. B*, 20(8):2291–2331.
19. Hsu, C. S. (1987). *Cell-to-cell mapping*, volume 64 of *Applied Mathematical Sciences*. Springer-Verlag, New York.
20. Hurley, M. (1995). Chain recurrence, semiflows, and gradients. *J Dyn Diff Equat*, 7(3):437–456.
21. Hurley, M. (1998). Lyapunov functions and attractors in arbitrary metric spaces. *Proc. Amer. Math. Soc.*, 126:245–256.
22. Iske, A. (1998). Perfect centre placement for radial basis function methods. Technical Report TUM-M9809, TU Munich, Germany.

23. Krauskopf, B., Osinga, H., Doedel, E. J., Henderson, M., Guckenheimer, J., Vladimirsky, A., Dellnitz, M., and Junge, O. (2005). A survey of methods for computing (un)stable manifolds of vector fields. *Internat. J. Bifur. Chaos Appl. Sci. Engrg.*, 15(3):763–791.
24. Lyapunov, A. M. (1992). The general problem of the stability of motion. *Internat. J. Control*, 55(3):521–790. Translated by A. T. Fuller from Édouard Davaux's French translation (1907) of the 1892 Russian original.
25. Wendland, H. (1998). Error estimates for interpolation by compactly supported Radial Basis Functions of minimal degree. *J. Approx. Theory*, 93:258–272.
26. Wendland, H. (2005). Scattered data approximation. Cambridge University Press, Cambridge.